IEEE Photonics Journal
An IEEE Photonics Society Publication

Nonlinear Impairment Compensation for Polarization-Division Multiplexed WDM Transmission Using Digital Backward Propagation

Volume 1, Number 2, August 2009

F. Yaman
Guifang Li, Senior Member, IEEE

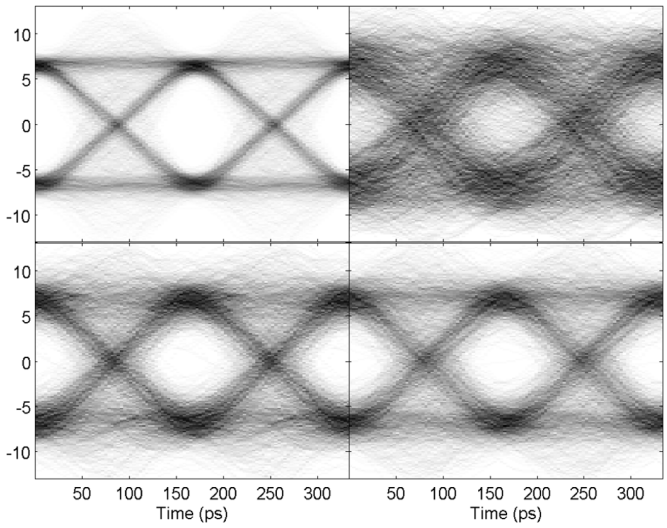

DOI: 10.1109/JPHOT.2009.2028157
1943-0655/$26.00 ©2009 IEEE

Nonlinear Impairment Compensation for Polarization-Division Multiplexed WDM Transmission Using Digital Backward Propagation

F. Yaman and Guifang Li, *Senior Member, IEEE*

CREOL, College of Optics and Photonics, University of Central Florida, Orlando, FL 32816 USA

DOI: 10.1109/JPHOT.2009.2028157
1943-0655/$26.00 ©2009 IEEE

Manuscript received June 8, 2009; revised July 12, 2009. First published Online July 21, 2009. Current version published August 7, 2009. Corresponding author: F. Yaman (e-mail: fyaman@creol.ucf.edu).

Abstract: It is shown experimentally that impairments induced by dispersion and Kerr nonlinearity can be compensated digitally for polarization-division multiplexed wavelength division multiplexing (WDM) transmission. The method of digital backward propagation based on solving the Manakov equation can be used to efficiently compensate for the nonlinear interactions between orthogonally polarized channels.

Index Terms: Coherent optical communication, polarization-mode dispersion, polarization-dependent loss, four-wave mixing.

1. Introduction

Recently, coherent detection opened new venues for long-haul optical communication systems. Among these are the possibility of using higher order modulation formats [1]–[4], the ability to pack channels more tightly using orthogonal frequency-division multiplexing and orthogonal wavelength-division multiplexing [5]–[7]. It was noticed early on that since coherent detection provided the complete information about the electric field including its intensity, phase and even polarization, the fiber-induced linear impairments such as dispersion could be eliminated using digital signal processing [8], [9]. Dispersion, being a linear and scalar impairment, can be compensated in a single step, which is commonly referred to as lumped compensation [10]–[17]. Subsequently it was shown that if the dispersion of the fiber was small enough, even the impairments caused by the Kerr nonlinearity which is often data dependent could be compensated [18]–[23]. However, in the more general case where both dispersion and nonlinearity have appreciable impact on the signal, these impairments cannot be removed in a single step. The accumulation of dispersion and nonlinearity and their impact on one another has to be followed throughout the transmission giving way to the distributed compensation [24]–[27]. Recently it was shown experimentally that the digital backward propagation (DBP) method based on solving the nonlinear Schrodinger (NLS) equation using the split-step method (SSM) can be used successfully to undo the combined effect of dispersion and nonlinearity [25], [28]. In the spirit of the SSM, DBP is distributed. However, in previous experimental demonstrations, all the channels had the same polarization, and solving the scalar nonlinear equation was adequate. In this paper, we demonstrate that the same principles can be applied to polarization-division multiplexed (PDM) wavelength division multiplexing (WDM) systems. The nonlinear interactions between channels that have the same polarization as well as different polarizations can be undone by solving the Manakov equation instead of the scalar NLS.

The major advantage of using digital compensation over all optical methods such as the mid-link optical phase conjugation is its flexibility. DBP does not require any symmetry on the link. The system parameters such as amplification scheme, amplifier spacing, dispersion or nonlinearity maps can be arbitrary, and can be changed arbitrarily over the lifetime of the link. Also, in the noiseless case, DBP can compensate all impairments exactly where as mid-link phase conjugation cannot.

In WDM systems, as the signal power is increased, individual channels suffer from self-phase modulation, and due to the presence of neighboring channels they suffer from cross-phase modulation and also four-wave mixing [29]–[34]. Self- and cross-phase modulation induce data-dependent chirp. Four-wave mixing on the other hand causes data-dependent power transfer between the channels. Because of dispersion, a given bit can interact with a number of bits in the other channels throughout the transmission. The combined effect of nonlinear interactions coupled with dispersion manifests as noise at the receiver. However, unlike the amplified spontaneous emission (ASE) noise, this noise is deterministic and therefore it can be removed given enough resources.

2. DBP for PDM WDM

The contribution of these nonlinear processes depends on several parameters such as signal power, fiber dispersion, channel spacing, and the state of polarization [32], [33]. If all the channels have the same polarization during transmission, dependence on polarization can be neglected as it was demonstrated in a recent experiment [28]. In this case, the scalar form of NLS describes the evolution of electric field in fibers [34]:

$$\frac{\partial A}{\partial z} = -\frac{\alpha}{2}A + \frac{i\beta_2}{2}\frac{\partial^2 A}{\partial t^2} + i\gamma|A|^2 A, \tag{1}$$

where A is the polarized electric field, α is the fiber loss, β_2 is the group velocity dispersion parameter, and γ is the nonlinearity parameter.

However, if all the channels do not have the same state of polarization as in the case of PDM or polarization interleaving, the effects of polarization on the nonlinear interactions have to be taken into account. Whether the total electric field is polarized or not, its propagation in a birefringence-free fiber can be described by the vectorial form of the NLS [34], [35]:

$$\begin{aligned}\frac{\partial A_x}{\partial z} &= -\frac{\alpha}{2}A_x + \frac{i\beta_2}{2}\frac{\partial^2 A_x}{\partial t^2} + i\gamma\left(|A_x|^2 + \frac{2}{3}|A_y|^2\right)A_x + \frac{i\gamma}{3}A_x^* A_y^2 \\ \frac{\partial A_y}{\partial z} &= -\frac{\alpha}{2}A_y + \frac{i\beta_2}{2}\frac{\partial^2 A_y}{\partial t^2} + i\gamma\left(|A_y|^2 + \frac{2}{3}|A_x|^2\right)A_y + \frac{i\gamma}{3}A_y^* A_x^2\end{aligned} \tag{2}$$

where A_x and A_y are the two orthogonal polarization components of the electric field. According to Eq. (2), the strength of the nonlinear processes, SPM, XPM and FWM depends on not only on the relative orientations of different channels but also on the state of polarizations. For instance, a channel polarized linearly accumulates more nonlinear phase due to SPM than another channel polarized elliptically [32], [33].

Optical transmission fibers are nominally not birefringent, however they still exhibit the so-called residual birefringence that randomly scatters the polarization of the electric field in lengths scales less than 100 m [36]. This polarization scattering length is much smaller than the nonlinear interaction length which is typically tens of kilometers. Since the polarization state of the electric field changes so fast, the resulting nonlinearity is not what is expected from a linearly polarized or circularly polarized field but an average over the entire Poincaré sphere. Averaging Eq. (2) over the fast polarization changes results in the Manakov equation given by [34], [36], [38]

$$\begin{aligned}\frac{\partial A_x}{\partial z} &= -\frac{\alpha}{2}A_x + \frac{i\beta_2}{2}\frac{\partial^2 A_x}{\partial t^2} + \frac{8i\gamma}{9}\left(|A_x|^2 + |A_y|^2\right)A_x \\ \frac{\partial A_y}{\partial z} &= -\frac{\alpha}{2}A_y + \frac{i\beta_2}{2}\frac{\partial^2 A_y}{\partial t^2} + \frac{8i\gamma}{9}\left(|A_y|^2 + |A_x|^2\right)A_y.\end{aligned} \tag{3}$$

The Manakov equation is simpler than the full vectorial NLS. Since the fast polarization rotations are averaged already, it is not necessary to follow these changes in the fiber. Moreover, since polarization changes are so fast and random, it does not matter anymore what the input polarization is. For instance, if only two channels propagate through the fiber, it does not matter whether both channels have linear polarization or circular polarization and the accumulated nonlinearity will be the same at the end of the fiber. However the strength of the nonlinear interaction still depends on the relative orientations of the channels. If the channels have the same polarization they interact more strongly than if they have orthogonal polarizations [39]. The Manakov equation as given in Eq. (3) assumes that the relative orientations of the polarizations of different channels remain the same throughout the fiber. This assumption is true as long as the bandwidth of the total field is narrow enough so that polarization-mode dispersion can be ignored, which is the case for the experiment described in this paper.

If the electric field is known at the transmitter side, the electric field at the end of the fiber can be obtained by solving the Manakov equation using the SSM [36], [34]. In this method, the propagation is divided into small steps such that after each step both the change in the spectrum through nonlinearity and the change in the instantaneous power profile through dispersion are small. In one step the Manakov equation is solved ignoring the nonlinear term, and in the next step it is solved ignoring the dispersion term. If the steps are small enough the electric field at the end of the fiber can be calculated with small error. The same procedure can be applied in the backward direction to obtain the electric field at the transmitter if the electric field can be measured at the receiver with adequate fidelity. This is the essence of the DBP method.

A consequence of the fast and random polarization rotations in the fiber is that, at the receiver the electric field is rotated with respect to the transmitter. To demultiplex the orthogonal channels properly, this random rotation has to be corrected. As these random rotations are slow, several electronic polarization demultiplexing methods based on digital signal processing have been devised to track these rotations and correct them [40]–[43]. However most of these methods are either data aided or Q-value directed and therefore they rely on high signal-to-noise ratio. Because of the linear and nonlinear impairments, the signal at the receiver end may be significantly distorted. This may make it difficult to separate the polarization multiplexed channels using the data-aided or Q-value-directed methods. However a closer look at the Manakov equation shows that it is not necessary to know at which polarization basis the data is encoded to implement backward propagation. This can be seen easily by verifying that the Manakov equation remains the same under the unitary transformation: $|A'\rangle = U|A\rangle$ where U is an arbitrary 2×2 unitary matrix, and $|A\rangle = [A_x \quad A_y]^T$ is the electric field in vectorial form. Therefore, DBP can be applied first and the electronic polarization demultiplexing techniques can be used subsequently to demultiplex the polarization channels correctly.

3. Experimental Setup

Fig. 1 shows the experimental setup. Three distributed-feedback lasers are used for the WDM channels. The central channel is set to 1550 nm. The total available bandwidth is limited to 24 GHz which is the double-sided analog bandwidth of the real-time oscilloscope. Using the OWDM concept, [6] made it possible to fit 3 WDM channels carrying 6 Gsymbols/s with a 7-GHz channel spacing into this bandwidth. A pattern generator is used to generate the BPSK data consisting of a pseudo-random bit sequence of length $2^{23} - 1$. The same data pattern is used to modulate all the channels and subsequently the central channel is delayed by several tens of bits with respect to the side channels. An RF delay is used to make sure that the bit slots for neighboring channels are aligned to maintain channel orthogonality [6]. WDM channels are combined with a 3-dB coupler with copies of the same signal at the two output ports. After delaying one arm with respect to the other and adjusting their polarizations the two copies are recombined with a polarizing beam combiner.

The PDM OWDM channels are launched into the loop controlled by two acousto-optic modulators. The loop consists of an 80-km-long nonzero dispersion-shifted fiber, an erbium-doped fiber amplifier (EDFA) followed by an ASE filter and a polarization controller. The fiber has a 0.2 dB/km loss, second- and third-order dispersion parameters of $\beta_2 = -4.84$ ps^2/km, $\beta_3 = 0.0812$ ps^3/km and nonlinearity parameter of $\gamma = 1.5$ W^{-1}km^{-1}. Polarization-mode dispersion parameter of the fiber is

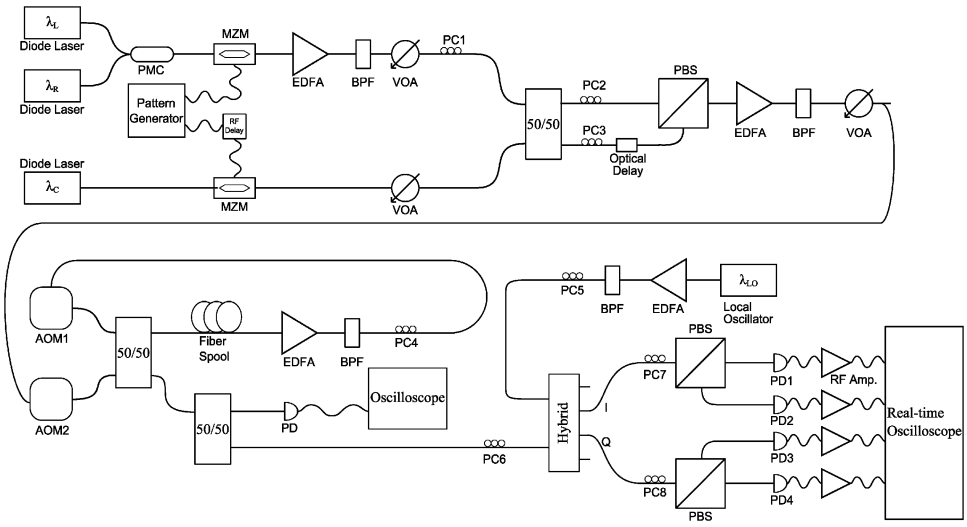

Fig. 1. Experimental setup for polarization-division multiplexed, three-channel OWDM, BPSK transmitter, loop and coherent polarization diversity receiver. PMC: polarization maintaining coupler, MZM: Mach–Zehnder modulator, EDFA: erbium-doped fiber amplifier, BPF: band-pass filter, PC: polarization coupler, PBS: polarizing beam splitter, VOA: variable optical attenuator, AOM: acousto optic modulator, PD: photodetector.

not measured, however, it is expected to be less than 0.1 ps$/\sqrt{\text{km}}$. A portion of the signal leaving the loop is monitored using an oscilloscope to make sure that loop loss is compensated by the amplifier gain. Power fluctuations between successive circulations could not be eliminated entirely because of the feedback nature of the loop.

At the receiver the signal is combined with the local oscillator at a 90° hybrid. The local oscillator wavelength is adjusted so that it coincided with the optical carrier of central channel. After the hybrid, each quadrature is separated into two orthogonal polarization components and detected by fast photodiodes. Since the hybrid ports had delays, balanced detection could not be used. Instead, the signal power was attenuated to 20 dB below the local oscillator power and the DC current after the detectors were removed by DC blocks. The local oscillator power had to be kept low enough ($<$ 2 mW) so that the responses of the photodiodes were linear. This required addition of amplifiers after the DC blocks to overcome the noise floor of the real-time oscilloscope. Three of the photodetectors has 3-dB bandwidths of 45 GHz, and the fourth has only 25 GHz. The amplifiers have 3-dB bandwidth at 25 GHz. The real-time oscilloscope has an analog bandwidth of 12 GHz which was extended to 16 GHz using the built-in digital filters.

The polarization controller following the LO (PC5) and the two controllers following the hybrid (PC7, PC8) are adjusted so that the polarization of the local oscillator makes 45° with the polarizing beam splitters, and power of the local oscillator measured at each port of the real-time oscilloscope are the same.

During transmission, because of the residual birefringence of the fibers and other components, polarization of the signal is rotated. This is equivalent to multiplying the signal with a unitary matrix. Several methods have been suggested for digitally estimating this matrix [40]–[43]. Since these methods are not the focus of this work, the polarization controller (PC6) is adjusted so that mixing between the two polarization channels is avoided. This is achieved by making sure that when only one polarization is launched into the loop no signal was collected at the second and fourth port of the real-time oscilloscope.

4. Experimental Results

The data collected by the real-time oscilloscope is sampled at 50 Gsample/s at each of the four ports simultaneously. The data from each port is saved and processed offline. The electric field at

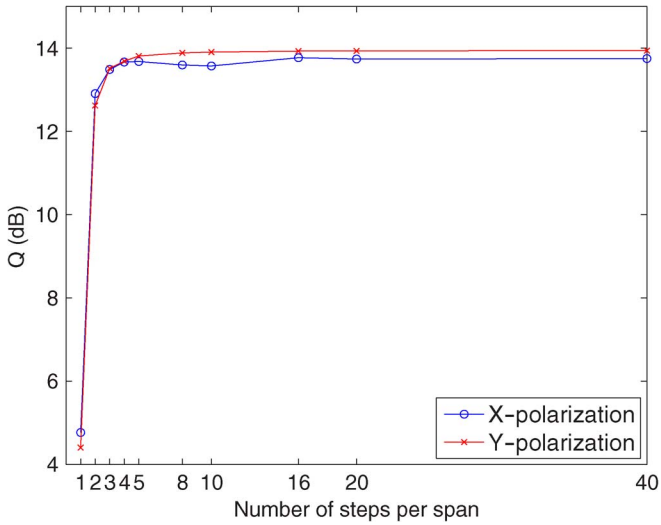

Fig. 2. Q value as a function of number of steps used per span.

the receiver is constructed form the saved data as

$$|A(L)\rangle = \begin{bmatrix} A_1 + iA_3 \\ A_2 + iA_4 \end{bmatrix} \tag{4}$$

where A_k with $k = 1 - 4$ are the data saved at the kth port of the real-time oscilloscope. The field at the transmitter $|A(0)\rangle$ is obtained by solving the Manakov equation in the backward direction using the symmetric SSM by putting $|A(L)\rangle$ as the input.

An important parameter of the back propagation is the step size. For backward propagation to work properly the step size should be small enough so that the impact of both nonlinearity and dispersion should be small in a single step [36]. Larger step size would induce error in the calculation and too small a step size would consume unnecessary amount of calculation. As a starting point the dispersion (L_D) and the nonlinear length (L_{NL}) can be calculated. These two parameters determine the length scale at which the signal is expected to be distorted significantly through dispersion and nonlinearity, respectively. For the SSM to work, the step size should be much smaller than both of these lengths. L_D and L_{NL} can be calculated from the fiber and signal parameters as $L_D = (\beta_2 \Delta f^2)^{-1}$, and $L_{NL} = L_{sp}[\gamma P_T \int_0^{L_{sp}} \exp(-\alpha z) dz]^{-1}$ where Δf is the total band width, L_{sp} is the span length, and P_T is the total power. With the parameters used in the experiment $\Delta f = 20$ GHz, $P_T = 4$ mW, $\gamma = 1.5$, L_D and L_{NL} are found to be 650 km and 630 km respectively. Therefore, the step size should be smaller than the span length. If the link parameters are changed the step size should be changed accordingly to maintain the accuracy of the SSM. For instance if standard single-mode fiber with a dispersion parameter of $\beta_2 = -21$ ps^2/km is used instead of nonzero dispersion-shifted fiber, the dispersion length would reduce to 150 km. Since the step size is determined by the smallest of the characteristic lengths, the computational load would increase approximately four times [27].

The step size can also be determined directly and more precisely by calculating the penalty in the Q value as a function of the step size. Fig. 2 shows the Q value obtained for the central channel after 960 km of transmission and DBP as a function of the number of steps used per span. When the step size is as small as 2 km, Q is close to 14 dB. Increasing the step size to 25 km does not change the Q value appreciably. However, if the step size is increased further, the error grows dramatically. Therefore, step size in the rest of the calculations are chosen to be 20 km.

To show that the Manakov equation would not be affected by a unitary rotation, $|A(L)\rangle$ is multiplied first with random unitary matrices U and after backward propagation $|A(0)\rangle$ is multiplied by U^{-1}. It is observed that the final results are identical, independent of the polarization rotation.

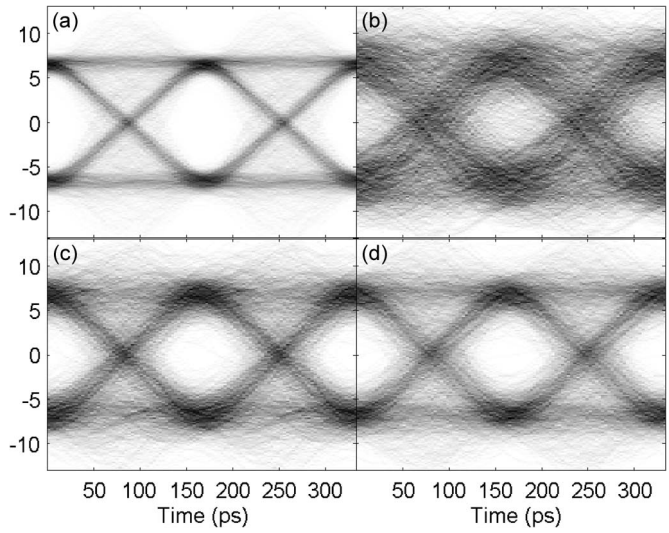

Fig. 3. Eye diagram for the central channel (a) at the transmitter and (b)–(d) after 1440 km. (b) Only dispersion compensation is used. (c) and (d) After back propagation for the x- and y-polarizations.

This shows that the DSP-based methods that rely on high signal quality can be used after backward propagation.

After backward propagation, the two polarization components are processed separately. The center channel is filtered using OWDM filtering and phase fluctuations stemming from carrier and local oscillator linewidth are removed using phase estimation. The decision threshold Q value [10] is calculated and used to estimate the effectiveness of back propagation.

Fig. 3(a) shows the back-to-back eye diagram for the central channel in the x-polarization corresponding to a Q value of 20.6 dB. The Q value for the y-channel is 19.7 dB. Fig. 3(b) and (c) are the eye diagrams obtained after 1440 km of transmission and subsequent DBP. In Fig. 3(b), only dispersion compensation is applied producing a Q value of 3.9 dB for the x-polarization. The eye is severely degraded and clearly dispersion is not the only source of impairment. Fig. 3(c) and (d), show the eye diagram for the x- and y-polarization after DBP. The eyes are still open and Q values for the two polarizations are 12.6 dB and 12.9 dB, respectively. DBP based on solving the Manakov equation can compensate for the dispersion and nonlinear impairments for both polarizations.

As the transmission distance increases, dispersion and nonlinearity accumulate and degrade the signal quality further. Moreover, with each additional span more ASE noise is added to the signal. The dependence of Q value as a function of transmission distance is measured and shown in Fig. 4. The Q values for both polarization channels after DBP using the Manakov equation are shown by the black curves. To show that the signal are impaired not only by dispersion but also by fiber nonlinearity, the Q values obtained by only applying dispersion compensation are also calculated and shown by the red curves. Comparison of the two cases show that at the power level used in the experiment the signal suffers from nonlinear impairments. It also shows that the nonlinear as well as the dispersive impairments are effectively removed by DBP.

To determine how much of the nonlinear impairment is caused by the presence of the orthogonally polarized channels, backward propagation is repeated using the scalar NLS (1) rather than the Manakov equation (3). All the parameters including dispersion, step size and nonlinearity coefficient are the same. The results are included in Fig. 4 with the blue curves. When the polarization effects are ignored, the nonlinear impairments cannot be compensated effectively, showing that the nonlinear processes depend on the polarization states of the interacting channels. It cannot be concluded from the comparison above that the majority of the nonlinear impairment stems from the nonlinear interactions of the orthogonal channels. This is because when scalar NLS is used for DBP the effects of nonlinear interactions between the channels having the same polarizations cannot be correctly compensated. As the nonlinear interactions happen between channels that have the same

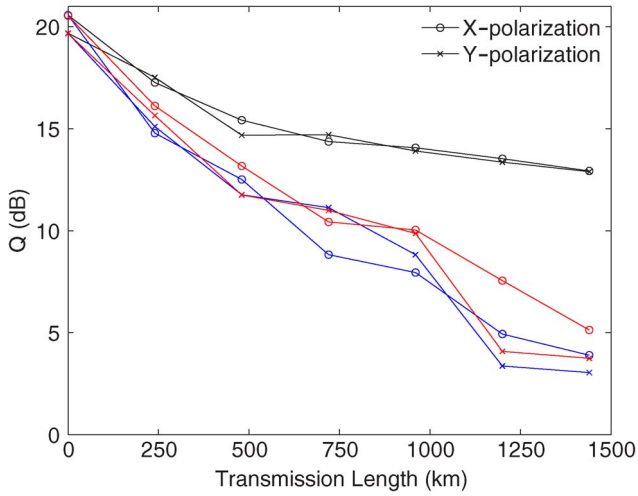

Fig. 4. Q values calculated every 240 km. The black curves are obtained after backward propagation solving the Manakov equation. The blue curves are obtained using the backward propagation, but scalar NLS is solved instead. The red curves are obtained by applying only dispersion compensation. Q values for the x- and y-polarizations are shown by circles and crosses.

polarizations and also between the channels that are orthogonal simultaneously, these effects have to be compensated simultaneously using the Manakov equation. Even when back propagation based on solving the Manakov equation is employed, the Q value drops as the propagation distance increases. The main reason for this drop is believed to be the accumulated ASE. As ASE is a nondeterministic noise source, it cannot be removed by DBP, which can only remove deterministic impairments. This is a fundamental limitation of the DBP method as it is applied in this experiment.

5. Conclusions and Discussions

The effectiveness of backward propagation relies critically on faithful recovery of the electric field at the receiver and also on determining the propagation parameters such as loss, dispersion, nonlinearity and power. The backward propagation should mimic the forward propagation closely. An error introduced at the receiver propagates and even grows because of the nonlinearity in backward propagation. As the ASE added to the signal at different spans cannot be measured, ASE further limits the performance of backward propagation.

After the deterministic distortions are compensated by DBP, the signal is expected to be limited by the Gordon–Mollenauer phase noise which is caused by conversion of ASE noise to phase noise through nonlinearity in both the forward and backward propagation. This limit is higher than the linear ASE limit if the total transmission length is larger than the nonlinear length [44]. DBP cannot remove the Gordon–Mollenauer noise completely however, it is expected to mitigate it [22].

The experimental setup presented in this Letter can be improved further especially at the receiver side. The use of balanced detectors would make it possible to use a local oscillator with power levels compared to the signal power. As a result the electrical signal after the photodiodes would be large enough and the amplifiers after the detectors which add additional noise and distortion can be avoided. The frequency response of the receiver is a combination of the detector, amplifier, and the real-time oscilloscope responses. The deviation of this response from a perfect rectangular shape introduces distortion on the signal which induces penalty on the backward propagation. Finally, because the experiment is setup in loop configuration, power fluctuations between the circulations could not be eliminated completely. As these fluctuations were not taken into account in the Manakov equation, the backward propagation could not remove the nonlinear impairments perfectly. Such fluctuations are expected to be smaller in a linear transmission setup.

The combined bandwidth of the channels was only 20 GHz, therefore polarization-mode dispersion is not expected to have an impact on the transmission. However, when the number of channels

is large, the channels at the opposite edges cannot retain their relative orientations because of polarization-mode dispersion. For DBP to work properly these changes in the forward propagation have to be measured and reproduced in backward propagation. This will require dynamic monitoring of the polarization transfer matrix of the transmission fiber.

References

[1] R. Noe, "Phase noise tolerant synchronous QPSK receiver concept with digital I&Q baseband processing," in *Proc. Opto-Electronics and Communications Conf. (OECC)*, Yokohama, Japan, Jul. 12–16, 2004, pp. 818–819.

[2] D. Ly-Gagnon, S. Tsukamoto, K. Katoh, and K. Kikuchi, "Coherent detection of optical quadrature phase-shift keying signals with carrier phase estimation," *J. Lightwave Technol.*, vol. 24, no. 1, pp. 12–21, Jan. 2006.

[3] A. H. Gnauck, P. J. Winzer, C. R. Doerr, and L. L. Buhl, "10 × 112-Gb/s PDM 16-QAM transmission over 630 km of fiber with 6.2-b/s/Hz spectral efficiency," in *Proc. OFC2009 PDPB8*, 2009.

[4] R. Dischler and F. Buchali, "Transmission of 1.2 Tb/s continuous waveband PDM-OFDM-FDM signal with spectral efficiency of 3.3 bit/s/Hz over 400 km of SSMF," in *Proc. OFC2009 PDPC2*, 2009.

[5] A. D. Ellis and F. C. G. Gunning, "Spectral density enhancement using coherent WDM," *IEEE Photon. Technol. Lett.*, vol. 17, pp. 504–506, 2005.

[6] G. Goldfarb, G. Li, and M. G. Taylor, "Orthogonal wavelength division multiplexing using coherent detection," *IEEE Photon. Technol. Lett.*, vol. 19, pp. 2015–2017, 2007.

[7] Q. Yang, N. Kaneda, X. Liu, S. Chandrasekhar, W. Shieh, and Y. Chen, "Real-time coherent optical OFDM receiver at 2.5-Gb/s for receiving a 54-Gb/s multi-band signal," in *Proc. OFC2009 PDPC5*, 2009.

[8] N. Takachio and K. Iwashita, "Compensation of fiber dispersion in optical heterodyne detection," *Electron. Lett.*, vol. 24, pp. 759–760, 1988.

[9] J. H. Winters and R. D. Gitlin, "Electrical signal processing techniques in long-haul, fiber-optic systems," *IEEE Trans. Commun.*, vol. 38, no. 9, pp. 1439–1453, Sep. 1990.

[10] M. G. Taylor, "Coherent detection method using DSP for demodulation of signal and subsequent equalization of propagation," *IEEE Photon. Technol. Lett.*, vol. 16, pp. 674–676, 2004.

[11] J. McNicol, M. O'Sullivan, K. Roberts, A. Comeau, D. McGhan, and L. Strawczynski, "Electrical domain compensation of optical dispersion [optical fibre communication applications]," in *Proc. Opt. Fiber Commun. Conf. Tech. Dig. OFC/NFOEC*, 2005, OThJ3.

[12] T. Pfau, S. Hoffmann, O. Adamczyk, R. Peveling, V. Herath, M. Porrmann, and R. Noé, "Coherent optical communication: Towards real-time systems at 40 Gbit/s and beyond," *Opt. Express*, vol. 16, pp. 866–872, 2008.

[13] S. Boehm, K. Schumacher, D. Goelz, and P. Meissner, "PMD compensation with coherent reception and digital signal processing," *Lasers and Electro-Optics*, 2007, CLEO 2007 JTuA132.

[14] A. T. Erdogan, A. Demir, and T. M. Oktem, "Automatic PMD compensation by unsupervised polarization diversity combining coherent receivers," *J. Lightwave Technol.*, vol. 26, no. 13, pp. 1823–1834, Jul. 1, 2008.

[15] S. J. Savory, G. Gavioli, R. I. Killey, and P. Bayvel, "Electronic compensation of chromatic dispersion using a digital coherent receiver," *Opt. Express*, vol. 15, pp. 2120–2126, 2007.

[16] C. Fludger, T. Duthel, T. Wuth, and C. Schulien, "Uncompensated transmission of 86 Gbit/s polarization multiplexed RZ-QPSK over 100 km of NDSF employing coherent equalisation," in *Proc. ECOC*, Sep. 2006.

[17] G. Charlet, J. Renaudier, M. Salsi, H. Mardoyan, P. Tran, and S. Bigo, "Efficient mitigation of fiber impairments in an ultra-long haul transmission of 40 Gbit/s polarization-multiplexed data by digital signal processing in a coherent receiver," in *Proc. OFC Conf.*, Mar. 2007.

[18] X. Liu, X. Wei, R. Slusher, and C. J. McKinstrie, "Improving transmission performance in differential phase-shift-keyed systems by use of lumped nonlinear phase-shift compensation," *Opt. Lett.*, vol. 27, pp. 1616–1618, 2002.

[19] K.-P. Ho and J. M. Kahn, "Electronic compensation technique to mitigate nonlinear phase noise," *J. Lightwave Technol.*, vol. 22, no. 3, pp. 779–783, Mar. 2004.

[20] G. Charlet, N. Maaref, J. Renaudier, H. Mardoyan, P. Tran, and S. Bigo, "Transmission of 40Gb/s QPSK with coherent detection over ultra-long distance improved by nonlinearity mitigation," in *Proc. Eur. Conf. Opt. Commun.*, Cannes, France, 2006.

[21] K. Roberts, L. Chuandong, L. Strawczynski, M. O'Sullivan, and I. Hardcastle, "Electronic precompensation of optical nonlinearity," *IEEE Photon. Technol. Lett.*, vol. 18, pp. 403–405, 2006.

[22] K. Kikuchi, "Electronic post-compensation for nonlinear phase fluctuations in a 1000-km 20-Gbit/s optical quadrature phase-shift keying transmission system using the digital coherent receiver," *Opt. Express*, vol. 16, pp. 889–896, 2008.

[23] L. B. Y. Du and A. J. Lowery, "Fiber nonlinearity precompensation for long-haul links using direct-detection optical OFDM," *Opt. Express*, vol. 16, pp. 6209–6215, 2008.

[24] R.-J. Essiambre, P. J. Winzer, X. Q. Wang, W. Lee, C. A. White, and E. C. Burrows, "Electronic predistortion and fiber nonlinearity," *IEEE Photon. Technol. Lett.*, vol. 18, pp. 1804–1806, 2006.

[25] E. Yamazaki, F. Inuzuka, K. Yonenaga, A. Takada, and M. Koga, "Compensation of interchannel crosstalk induced by optical fiber nonlinearity in carrier phase-locked WDM system," *IEEE Photon. Technol. Lett.*, vol. 19, pp. 9–11, 2007.

[26] X. Li, X. Chen, G. Goldfarb, E. Mateo, I. Kim, F. Yaman, and G. Li, "Electronic post-compensation of WDM transmission impairments using coherent detection and digital signal processing," *Opt. Express*, vol. 16, pp. 880–888, 2008.

[27] E. Mateo, L. Zhu, and G. Li, "Impact of XPM and FWM on the digital implementation of impairment compensation for WDM transmission using backward propagation," *Opt. Express*, vol. 16, pp. 16 124–16 137, 2008.

[28] G. Goldfarb, M. G. Taylor, and G. Li, "Experimental demonstration of fiber impairment compensation using the split-step finite-impulse-response filtering method," *IEEE Photon. Technol. Lett.*, vol. 20, pp. 1887–1889, 2008.

[29] D. Marcuse, A. R. Chraplyvy, and R. W. Tkach, "Effect of fiber nonlinearity on long-distance transmission," *J. Lightwave Technol.*, vol. 9, no. 1, pp. 121–128, Jan. 1991.
[30] R. W. Tkach, A. R. Chraplyvy, F. Forghieri, A. H. Gnauck, and R. M. Derosier, "Four-photon mixing and high-speed WDM systems," *J. Lightwave Technol.*, vol. 5, no. 5, pp. 841–849, May 1995.
[31] N. Kikuchi, K. Sekine, and S. Sasaki, "Analysis of cross-phase modulation effect on WDM transmission performance," *Electron. Lett.*, vol. 33, pp. 653–654, 1997.
[32] Q. Lin and G. P. Agrawal, "Vector theory of cross-phase modulation: Role of nonlinear polarization rotation," *IEEE J. Quantum Electron.*, vol. 40, no. 7, pp. 958–964, Jul. 2004.
[33] M. Karlsson and H. Sunnerud, "Effects of nonlinearities on PMD-induced system impairments," *J. Lightwave Technol.*, vol. 24, no. 11, pp. 4127–4137, Nov. 2006.
[34] G. P. Agrawal, *Nonlinear Fiber Optics,* 3rd ed. San Diego, CA: Academic, 2001.
[35] B. Crosignani and P. Di Porto, "Intensity induced rotation of the polarization ellipse in low-birefringence, single mode optical fibres," *Opt. Acta*, vol. 32, pp. 1251–1258, 1985.
[36] D. Marcuse, C. R. Menyuk, and P. K. A. Wai, "Application of the Manakov-PMD equation to studies of signal propagation in optical fibers with randomly varying birefringence," *J. Lightwave Technol.*, vol. 15, no. 9, pp. 1735–1746, Sep. 1997.
[37] C. D. Poole and R. E. Wagner, "Phenomenological approach to polarization dispersion in long single-mode fibers," *Electron. Lett.*, vol. 22, pp. 1029–1030, 1986.
[38] P. K. A. Wai, W. L. Kath, C. R. Menyuk, and J. W. Zhang, "Nonlinear polarization-mode dispersion in optical fibers with randomly varying birefringence," *J. Opt. Soc. Amer. B*, vol. 14, pp. 2967–2979, 1997.
[39] C. McKinstrie, H. Kogelnik, R. Jopson, S. Radic, and A. Kanaev, "Four-wave mixing in fibers with random birefringence," *Opt. Express*, vol. 12, pp. 2033–2055, 2004.
[40] Y. Han and G. Li, "Coherent optical communication using polarization multiple-input-multiple-output," *Opt. Express*, vol. 13, pp. 7527–7534, 2005.
[41] M. T. Core, "Cross polarization interference cancellation for fiber optic systems," *J. Lightwave Technol.*, vol. 24, no. 1, pp. 305–312, Jan. 2006.
[42] T. Pfau, R. Peveling, S. Hoffmann, S. Bhandare, S. Ibrahim, D. Sandel, O. Adamczyk, M. Porrmann, R. Noé, Y. Achiam, D. Schlieder, A. Koslovsky, Y. Benarush, J. Hauden, N. Grossard, and H. Porte, "PDL-tolerant real-time polarization-multiplexed QPSK transmission with digital coherent polarization diversity receiver," in *Proc. SUM2007*, Portland, OR, Jul. 23–25, 2007, Ma3.3.
[43] H. Zhang, Z. Tao, L. Liu, S. Oda, T. Hoshida, and J. C. Rasmussen, "Polarization demultiplexing based on independent component analysis in optical coherent receivers," in *Proc. 34th Eur. Conf. Opt. Commun.*, 2008.
[44] J. P. Gordon and L. F. Mollenauer, "Phase noise in photonic communications systems using linear amplifiers," *Opt. Lett.*, vol. 15, pp. 1351–1353, 1990.